**Journal of NeuroVirology,** 16: 318–329, 2010

ISSN 1355-0284 print / 1538-2443 online
DOI: 10.3109/13550284.2010.501847

informa
healthcare

# Neurological suppression of diaphragm electromyographs in hamsters infected with West Nile virus

John D Morrey,[1] Venkatraman Siddharthan,[1] Hong Wang,[1] Jeffery O Hall,[1] Neil E Motter,[1] Robert D Skinner,[2] and Ramona T Skirpstunas[1]

*[1]Institute for Antiviral Research, Department of Animal, Dairy, and Veterinary Sciences, Utah State University, Logan, Utah, USA; and [2]Center for Translational Neuroscience and Department of Neurobiology and Developmental Sciences, University of Arkansas for Medical Sciences, Little Rock, Arkansas, USA*

**To address the hypothesis that respiratory distress associated with West Nile virus (WNV) is neurologically caused, electromyographs (EMGs) were measured longitudinally from the diaphragms of alert hamsters infected subcutaneously (s.c.) with WNV. The EMG activity in WNV-infected hamsters was consistently and significantly ($P \leq .001$) less than that of sham-infected animals, beginning with suppression at day 3 and continuing to beyond day 17 after viral challenge. Of the tissues known to affect respiration, i.e., lung, diaphragm, cervical spinal cord, brain stem, and the carotid or aortic bodies, foci of WNV-immunoreactive neurons were only observed in the brain stems and some cervical spinal cords from EMG-suppressed animals. To confirm the involvement of the brain stem and spinal cord, WNV was injected directly in the ventrolateral medulla containing respiratory functions using stereotaxic surgery and into the cervical cord at the C4 vertebral level. As with subcutaneous WNV challenge, hamsters developed EMG suppression of the diaphragm within 4 days. Because WNV-positive neurons were only sporadically identified in EMG-suppressed animals as early as day 3, a plausible mechanism of EMG suppression may involve regulation of diaphragm activity via vagal afferents acting on respiratory control system neurons in the brain stem. Brain auditory evoked response (BAER) was performed to determine if generalized brain stem neuropathy was the cause of diaphragmatic EMG suppression. Because deficiencies of BAER were only observed after day 11, which is long after diaphragm EMGs became suppressed, multiple phases of WNV-induced neurological disease are likely. These data establish that WNV infection of hamsters causes electrophysiological suppression of the diaphragm either directly by lesions in the brain stem and cervical spinal cord, or indirectly by altered vagal afferent function. This WNV-induced EMG suppression may be analogous to conditions leading to respiratory distress of WNV-infected human patients.** *Journal of NeuroVirology* (2010) **16,** 318–329.

**Keywords:** brain stem; diaphragm; electromyography; spinal cord; West Nile virus

Address correspondence to John D. Morrey, PhD, Institute for Antiviral Research, Department of Animal, Dairy, and Veterinary Sciences, Utah State University, 4700 Old Main Hill, Logan, UT 84341, USA. E-mail: john.morrey@usu.edu

This work was supported by N01-AI-30063, Virology Branch, NIAID, NIH (J.D.M.); grant 1 U54 AI-065357-04, Rocky Mountain Regional Centers of Excellence, NIAID, NIH (J.D.M.); and grant RR020146, NIH (R.D.S). The authors give special thanks to Andy Christensen for animal experiments, Alex Wouden for software design for plethysmography and EMG, Jacob Brown and Alex Wouden for software design of BAER, Ashley Dagley for performing BAER, and Walter M. St. John, Emeritus Professor of Physiology, Dartmouth School of Medicine, for helpful suggestions on lung physiology. The authors are also grateful for encouragement from James J. Sejvar, neuroepidemeologist at the US Center for Disease Control and Prevention, to investigate respiratory functions in WNV-infected animals.

Received 21 April 2010; revised 28 May 2010; accepted 8 June 2010.

## Introduction

Respiratory distress has been described in West Nile virus (WNV)-infected patients with neurological disease, including those with acute flaccid paralysis (Fratkin *et al,* 2004; Sejvar *et al,* 2006). Four of 12 patients who died from WNV infection in Mississippi in the year 2002 with postmortem examinations presented with varied symptoms, but each person had respiratory failure that required intubation and ventilation (Fratkin *et al,* 2004). Because histopathology was observed in the gray matter ventral horn gray matter of the spinal cord, the brain stem, cerebellum, and cerebrum, the cause of respiratory failure was presumptively considered to be neurologic.

A cohort of 32 patients with WNV-induced paralysis was followed up 4 months (Sejvar *et al,* 2005) and 1 year later (Sejvar *et al,* 2006). At 4 months, three patients with respiratory failure had died and two were intubated. By 1 year, three of the additional cohorts who had died, all had respiratory failure. At 1 year, some of the remaining cohorts continued to have respiratory involvement, including a need for supplemental oxygen, intubation, orthopnea, and/or dyspnea on exertion and weakness of cough.

From such clinical observations, it can be concluded that WNV presumptively causes lesions in the central nervous system (CNS) that adversely affect pulmonary function. Because WNV destroys (Chu and Ng, 2003; Samuel *et al,* 2006; Shrestha *et al,* 2003) or persistently infects motor neurons (Siddharthan *et al,* 2009; Siirin *et al,* 2007; Tonry *et al,* 2005; Wu *et al,* 2008) in cell culture or in the spinal cord of rodents to cause muscle weakness and paralysis, lesions in the spinal cord might also affect respiratory function. The diaphragm is innervated by phrenic nerves whose cell bodies reside at C3–C5 in the cervical cord. So if motor neurons in the C3–C5 were damaged or destroyed by WNV, innervation of the diaphragm would decrease. Additionally, WNV infects and causes lesions in the brain stem of human patients (Doron *et al,* 2003; Petropoulou *et al,* 2005) and other species (Cantile *et al,* 2001; Siddharthan *et al,* 2009), which contains respiratory control functions in the medulla and pons (Dubreuil *et al,* 2009; Okada *et al,* 2009; Rudzinski and Kapur, 2009). Afferent axons from the carotid and aortic bodies in the glossopharyngeal nerve contain chemoreceptor cells and vagal afferent nerves from receptors in the lung (Goehler *et al,* 2005, 2006; Hermann and Rogers, 2009) communicate with the medulla and pons respiratory control centers to coordination inspiration and expiration. Therefore, WNV-induced lesions in the respiratory control centers or WNV-induced alteration of signaling from vagal afferents could also adversely affect respiration.

Hamsters infected with WNV manifest similar neurological disease signs as observed in human patients (Morrey *et al,* 2004, 2007, 2008; Siddharthan *et al,* 2009), among those being paralysis caused by infection of the gray matter of the spinal cord. Because lesions in the gray matter of the spinal cord or in the brain stem could presumptively cause respiratory distress, we employed these animal models to investigate the pathogenesis of respiratory dysfunction caused by WNV.

## Results

To address the hypothesis that WNV-induced respiratory distress is neurologically caused, electromyographs (EMGs) were measured longitudinally from the diaphragms of alert hamsters infected subcutaneously (s.c.) with WNV. In agreement with the hypothesis, the WNV-injected hamsters developed dysfunctional EMG tracings (Figure 1B, D), as measured by suppressed root-mean-square (RMS) values of the EMG amplitude (Figure 1A, C) over the time course of infection. The EMGs of WNV-infected animals were statistically different from the sham-infected animals ($P \leq .001$) (Figure 1A, C). These data established that WNV s.c. injection causes EMG suppression of the diaphragm.

To establish that suppression of diaphragmatic EMG is not due to a universal viral infection response, hamsters were injected with Pichinde virus, an arenavirus causing hemorrhagic fever in hamsters, but not central nervous system infection (Gowen *et al,* 2008). The same day of infection, EMG wires were surgically implanted in the diaphragm and EMG readings were recorded on days 2 to 6 after infection. None of the three Pichinde virus-infected animals had suppressed EMGs up to 6 days after viral challenge, in contrast to those observed with WNV infection (Figure 2). The EMGs were recorded up through the severe stages of disease when animal started succumbing to disease at day 7.

To investigate lesions that might be responsible for EMG suppression, tissues known to control respiration were collected from subcutaneously WNV-injected animals when they first developed suppressed EMGs (day 3) (Figure 3A) and after they had sustained EMG suppression at days 7 and 8 (Figure 3B) (Table 1). The tissues were lung, diaphragm, cervical spinal cord, brain stem, or the carotid and aortic bodies sensing pH, $O_2$, and $CO_2$ (Focosi *et al,* 2007; Gonzalez *et al,* 1994). WNV-positive immunostaining or histopathology was observed only in the brain stems or cervical spinal cords, but not in the other tissues. WNV-positive immunostained foci were identified in brain stems from all four animals with suppressed EMGs assayed 7 and 8 days after challenge; whereas, the cervical cords from two of four animals at that time were negative for the WNV protein (Table 1). Likewise, all four animals had histological changes in the brain stem, but only one animal (no. 301) possessed

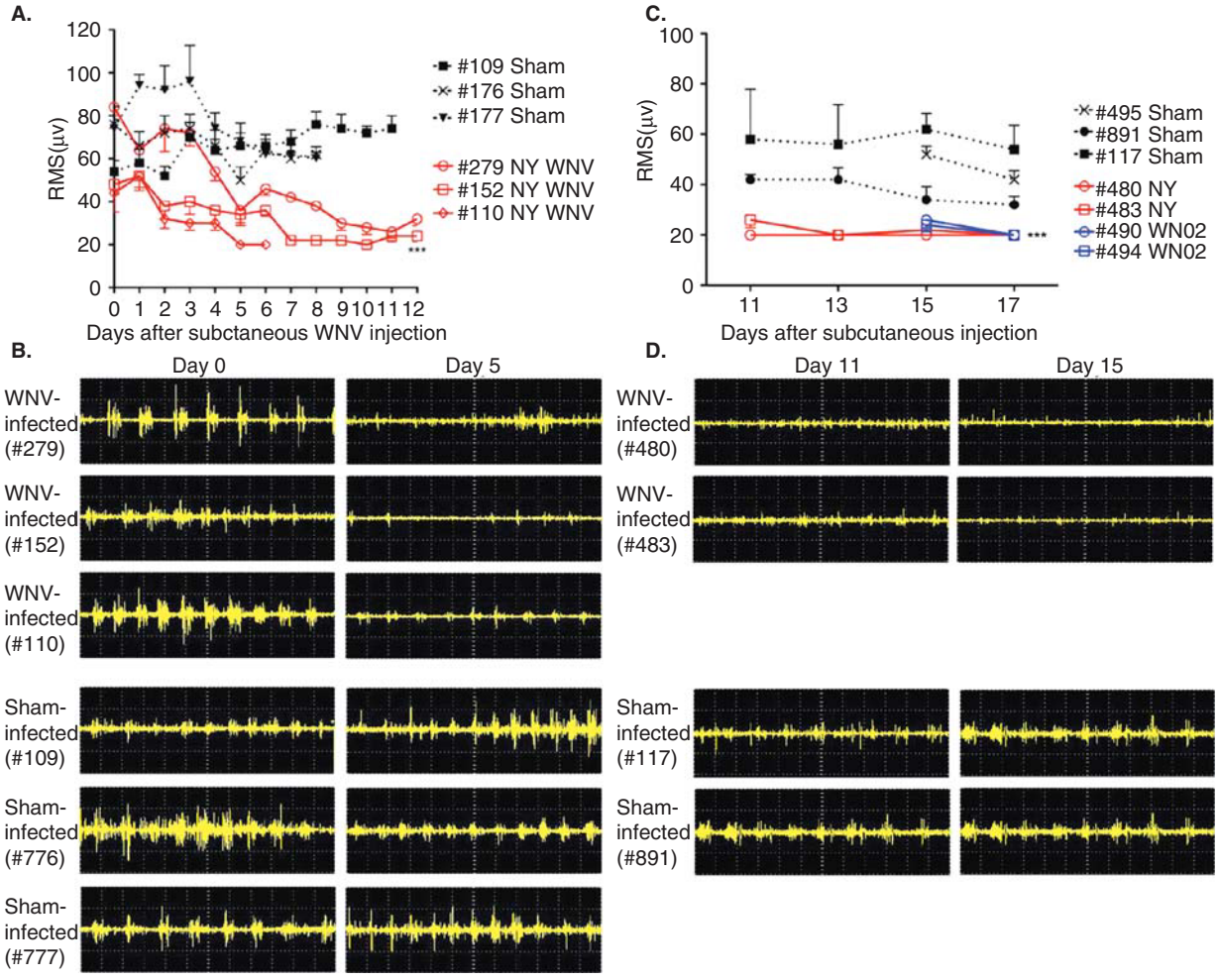


**Figure 1** Electromyography (EMG) from diaphragms of hamsters injected subcutaneously with NY WNV (5. $3 \times 10^5$ PFU) or WN02 ($2.8 \times 10^3$ PFU). (**A, C**) Root-mean-square (RMS) of EMG amplitudes. Each data point was the mean ± SD of 10 consecutive EMG recordings of 1.2 s each. (**B, D**) Representative raw EMG recordings. (**A, B**) RMS at days 0 to 12 with three sham- and three WNV-infected hamsters and (**C, D**) days 11 to 17 after viral challenge with three sham- and four WNV-infected hamsters. EMG was performed in alert unanesthetized animals. ***$P \leq .001$ compared to sham-infected data using two-way ANOVA (Prism 4 for Macintosh; GraphPad Software) of data between days (**A**) 3 and 6 or (**B**) 11 and 17.

such pathology in the cervical spinal cord (Figure 3). Examples of the histology from the brain stem and cervical cord are shown for animals challenged with WNV in the cervical cord, medulla, and subcutaneously (Figure 4). Pathology in the brain stem and cervical cord included lymphocytic infiltration and perivascular cuffing. The cervical cord also included infrequent axonal swelling and gliosis.

No WNV-positive immunostained foci or histopathology was observed in the brain stem or cervical cord from the one EMG-suppressed animal (no. 455) on day 3 (Table 1, Figure 3). Positive foci of infection may have been missed in this animal, however, because the complete brain stem was not sectioned for analysis and positive foci of infection have been observed at day 3 in another WNV-infected hamster (data not shown). These data establish that rare WNV-immunostained foci can sometimes be located in the brain stem, but not in the cervical cord, as early as day 3 after viral challenge. However, positive WNV-immunostained foci with histopathology were uniformly observed in the brain stems of hamsters with suppressed EMGs at days 7 and 8 (Table 1). Cervical cord infections and histopathology were observed in some, but not all of these EMG suppressed animals.

Hamsters were injected with WNV directly into the medulla to determine if lesions specifically in this anatomical location could cause EMG suppression. EMGs were recorded longitudinally from the diaphragm in a hamster (no. 29) injected bilaterally into the medulla with WNV (WN02) or in a hamster sham-injected (no. 67) (Figure 5). Two other hamsters were repeated on another day (trial 2). Sample EMG recordings from WNV-injected hamsters from both Trials 1 and 2 were (Figure 5B) markedly suppressed beginning early in the course of infection ($P \leq .001$). The root-mean-square (RMS) values from

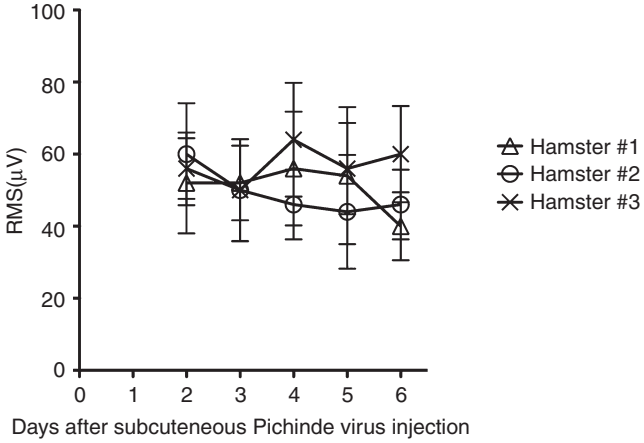


**Figure 2** Electromyography (EMG) of diaphragms from three hamsters injected subcutaneously with Pichinde virus. Each data point was the mean root-mean-square (RMS) ± SD of 10 EMG measurements. EMG was performed in alert unanesthetized animals. Hamsters started succumbing to disease on day 7.

the two WNV-injected hamsters were significantly suppressed over the course of the experiment ($P \leq .001$) (Figure 5A). The raw EMGs or their RMS values were not suppressed in sham-injected animals. These data demonstrated that WNV injection in the medulla oblongata resulted in EMG suppression. In another set of animals, tissues were collected from animals directly injected with WNV bilaterally into the medulla or in C5 of the cervical cord (Table 1, Figure 3C, D). EMG-suppressed animals (nos. 406, 452) injected with WNV in the cervical cord and the medulla, respectively, both had WNV-positive foci and histopathology in the brain stems and the cervical spinal cords.

No WNV-immunoreactive cells or histopathological lesions were identified in the lung of EMG-suppressed animals to suggest degradation of alveoli sacks that could account for any pulmonary dysfunction (Table 1). Likewise, none of the diaphragms, carotid bodies, or aortic bodies possessed WNV-immunoreactive cells or histopathology (data not shown).

Brain auditory evoked response (BAER) was used to assess the presence of generalized lesions in the brain stem. Because the auditory pathway extends oven much of the brain stem, this assay was selected to determine if generalized brain stem neuropathy was the cause of diaphragmatic EMG suppression. In alert anesthetized animals and humans, auditory clicks evoke electrical potentials with different latencies as the induced signal progresses along the auditory pathway through the pons and midbrain. Prominent peaks in the BAER represent evoked activity in the ventral cochlear nucleus (peak I), the superior olivary nucleus (peak III), and the lateral lemniscus (peak V) in the brain stem. Besides providing an assessment of threshold, BAERs can be used to monitor the auditory pathway in the brain stem by measuring the latencies of peaks III and V, where peak I is used as a reference point (Hoffman and Horowitz, 1984; Jiang *et al,* 2009). These peaks were identified in normal hamsters using diminishing decibels (db) of sound (Figure 6A). To evaluate the brain stem function of WNV-infected hamsters, the latencies between peaks I and III, I and V, and III and V were measured on days 7 and 11 (Figure 6B). No statistical differences were observed between WNV- and sham-infected animals up to 7 days post infection; however, the BAERs of some WNV-infected animals only at day 11 (not day 7) were qualitatively abnormal so that accurate peak measurements could not be made (see Figure 6B). Examples of WNV-induced abnormal BAERs (nos. 260, 349, 126) obtained at day 11, along with a normal BAER from a sham-infected hamster (no. 256), are shown in Figure 6C. At day 11, all of the 15 sham-injected hamsters were normal, but 3 of 12 WNV-injected hamsters were abnormal. The lack of abnormal BAER data early in the course of infection when EMGs were suppressed suggests that the lesions causing suppression of EMG were not the same as the lesions causing BAER abnormalities. Because BAER abnormality at day 11 probably detected generalized neuropathy in the brain stem, EMG suppression as early as day 3 was not likely cause by generalized neuropathy.

## Discussion

Based upon respiratory distress and failure observed in some WNV-infected human patients (Fratkin *et al,* 2004; Sejvar *et al,* 2006), we addressed the hypothesis that respiratory distress is caused by lesions in the central nervous system. EMGs measured in the diaphragms of infected rodents were used to test this hypothesis. We reasoned that deficiencies in the diaphragmatic EMG could reflect deficiencies in other neurologically controlled functions, e.g., the medullary chemoreceptor/respiratory neurons, respiratory afferent nerve fibers including the vagus nerve, respiratory nuclei in the medulla and pons and tracts to the spinal cord, cervical motor neurons, and the phrenic nerve. To longitudinally measure diaphragmatic EMG, an electrode was implanted in the midcostal region in one side of the diaphragm in unanesthetized hamsters. Ten consecutive recordings were made and the average root-mean-square (RMS) of EMG waveform was calculated. Because the animals were alert, breathing rates were variable; nevertheless, we were able to quantifiably measure suppressed EMG amplitudes of infected animals.

All animals challenged subcutaneously with WNV, in the ventrolateral medulla, or in the cervical spinal cord eventually developed suppressed EMGs as compared to no suppression in sham-infected animals. WNV-induced EMG suppression could theoretically be affected by infected tissues

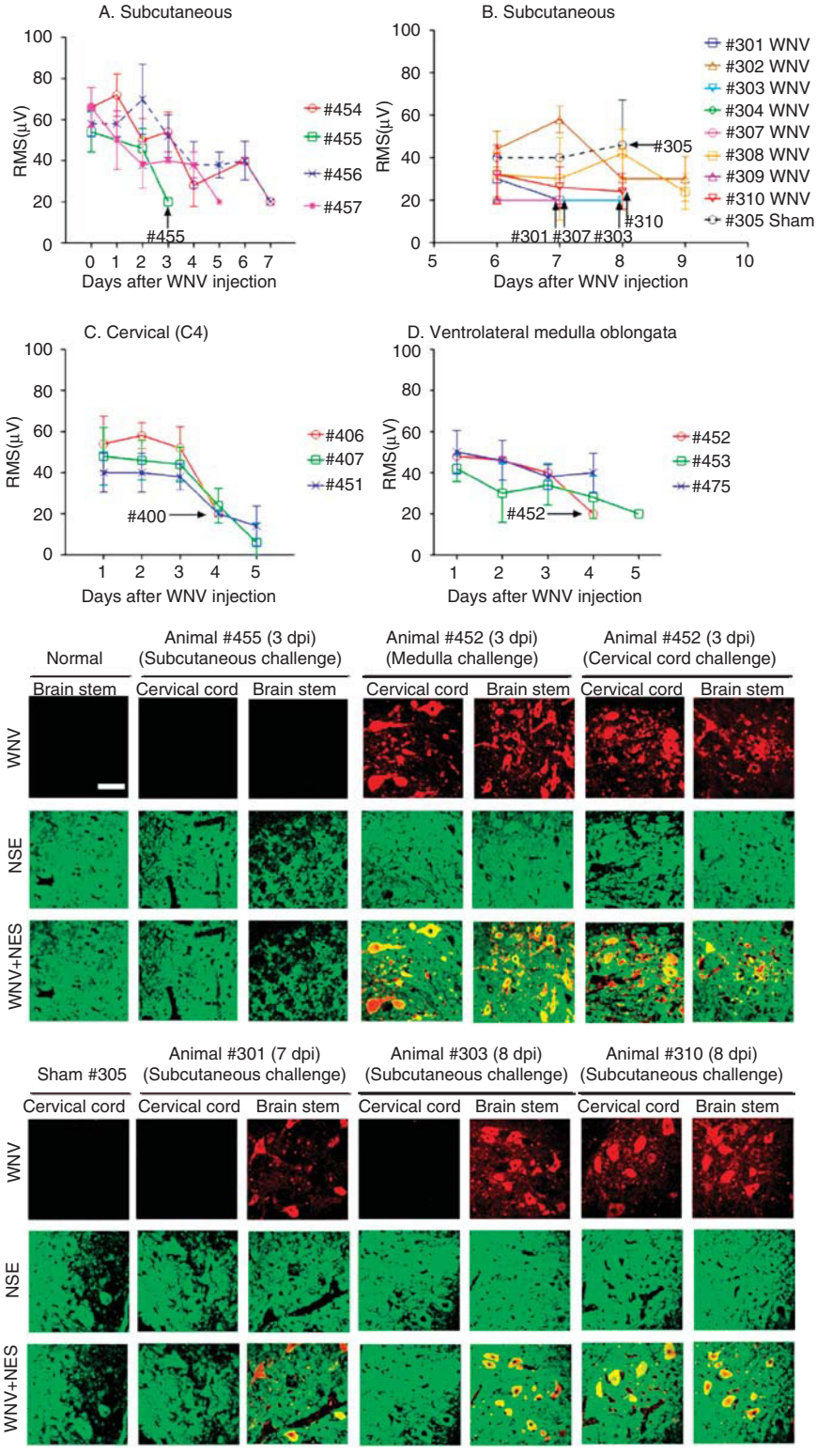


**Figure 3** Diaphragmatic electromyography amplitudes converted to root mean square (RMS) at various days after (**A, B**) subcutaneous (12 WNV-injected, 1 sham-injected), (**C**) cervical spinal cord (3 WNV-injected), or (**D**) ventrolateral medulla challenge (on both sides) with WNV in three hamsters. Necropies were performed on days 3 (no. 455), 4 (nos. 406, 452), 7 (nos. 301, 307), and 8 (nos. 303, 310, 305) after viral challenge. Confocal immunohistochemistry for WNV envelope (WNV) and neuron-specific enolase (NSE) (lower panels) was performed on brain stems and cervical spinal cords when EMGs first became suppressed. Animals necropsied on or before day 5 (**A, B, C**) were challenged with NY WNV. Animals necropsied after day 5 were challenged with WN02. Confocal microscopy scale bar = 20 μM.

**Table 1** WNV immunohistochemistry and histopathology of the cervical cords, brain stems, and lungs from hamsters possessing suppressed diaphragmatic electromyograms (EMGs) (see Figure 3) at various days after subcutaneous, cervical spinal cord, or bilateral ventrolateral medulla challenge (both sides) with WNV (NY WNV on 3 to 4 dpi; WN02 on 7 to 8 dpi)

| | | | Brain stem | | Cervical cord | | Lung |
|---|---|---|---|---|---|---|---|
| Hamster no. | Challenge route | Days post injection | WNV immunohistochemistry | Histopathology (H&E) | WNV immunohistochemistry | Histopathology (H&E) | WNV immunohistochemistry |
| 455 | Subcutaneous | 3[a] | Neg (HRP & CF) | Neg | Neg (HRP & CF) | Neg | Neg (HRP) |
| 406 | Cervical | 4 | Pos (AP & CF) | Histopath | Pos (AP & CF) | Histopath | Neg (HRP) |
| 452 | Medulla | 4 | Pos (AP & CF) | Histopath | Pos (AP & CF) | Histopath | Neg (HRP) |
| 301 | Subcutaneous | 7 | Pos (HRP & CF) | Histopath | Neg (HRP & CF) | Histopath | ND |
| 307 | Subcutaneous | 7 | Pos (HRP & CF) | Histopath | Pos (HRP & CF) | Neg | Neg (HRP) |
| 303 | Subcutaneous | 8 | Pos (HRP & CF) | Histopath | Neg (HRP & CF) | Neg | Neg (HRP) |
| 310 | Subcutaneous | 8 | Pos (HRP & CF) | Histopath | Pos (HRP & CF) | Neg | Neg (HRP) |
| 305, Sham | Subcutaneous | 8 | Neg (HRP & CF) | Neg | Neg (HRP & CF) | Neg | Neg (HRP) |

*Note.* Neg = negative for WNV-immunostained cells or histopathology; Pos = positive for WNV-immunostained cells; Alk phos = Alkaline phosphatase immunostaining was used; HRP = horseradish peroxidase immunostaining was used; CF = confocal microscopy was used; Histopath = histopathology, includes lymphocytic infiltration, perivascular cuffing, axonal swelling, gliosis. ND = not done.[a]Another animal having $SaO_2$ suppression 3 days after s.c. viral challenge also had the same WNV-immunohistochemical and histopathological results.

regulating respiration such as the diaphragm, carotid and aortic bodies, medulla/pons, cervical spinal cord, and the lung. Foci of viral infected cells detected by immunohistochemistry, however, were only observed in the cervical cord, and most consistently, in the brain stem. Lesions in the diaphragm could theoretically cause EMG suppression; however, this does not seem likely because we did not observe WNV-infected cells or histopathology from hematoxylin and eosin (H&E) examination in the diaphragm (data not shown). Direct infection of the lung would not likely affect diaphragmatic EMGs, which was consistent with a lack of correlation of lung infection or histopathology with EMG suppression.

Another possible cause of WNV-induced EMG suppression is cytokine signaling of the vagal afferent nerves to central autonomic pathways (Goehler *et al,* 2005, 2006; Hermann and Rogers, 2009). Multiple pathways and mechanisms have been described for the communication from the immune system to the central nervous system. For example, local cytokines due to infections within terminal fields of peripheral sensory nerves can result in early cytokine-induced signaling to the central autonomic system, although no examples on the effect of autonomic EMG function by cytokine signaling has yet been described. Circulating cytokines can also alter vagal afferent signaling of autonomic control (Goehler *et al,* 2005). The observation that EMG suppression can occur early after viral challenge before extensive WNV infection and pathology in the brain stem suggests that the mechanism of EMG suppression involves peripheral immune communication to the central nervous system. Two findings, however, argue against this mechanism of action, but do not rule it out. One finding is that the EMG suppression is sustained through the course of disease out to day 17 or beyond, whereas cytokine or innate immunity fluctuates over time. The other finding is that a viral infection of hamsters with Pichinde virus causing systemic, but not neurologic disease, did not affect EMGs.

Also supporting the hypothesis that lesions in the medulla or cervical cord can cause respiratory dysfunction are prior reports. Evidence that disease of the medulla can cause respiratory distress are congenital central hypoventilation syndrome (Gaultier *et al,* 2004; Rudzinski and Kapur, 2010) or severe brain injury (Woischneck *et al,* 2009), which results in damage to medullar respiratory control function. More relevant to WNV infection is bulbar poliomyelitis in which poliovirus infects the medulla oblongata to cause respiratory dysfunction. Bulbospinal poliomyelitis is the infection of both the medulla and the cervical (C3–C5) spinal cord to cause paralysis of the diaphragm (Atkinson *et al,* 2007).

Infectious titers or WNV-specific polymerase chain reaction (PCR) from homogenized tissues were not utilized to detect virus in the brain or

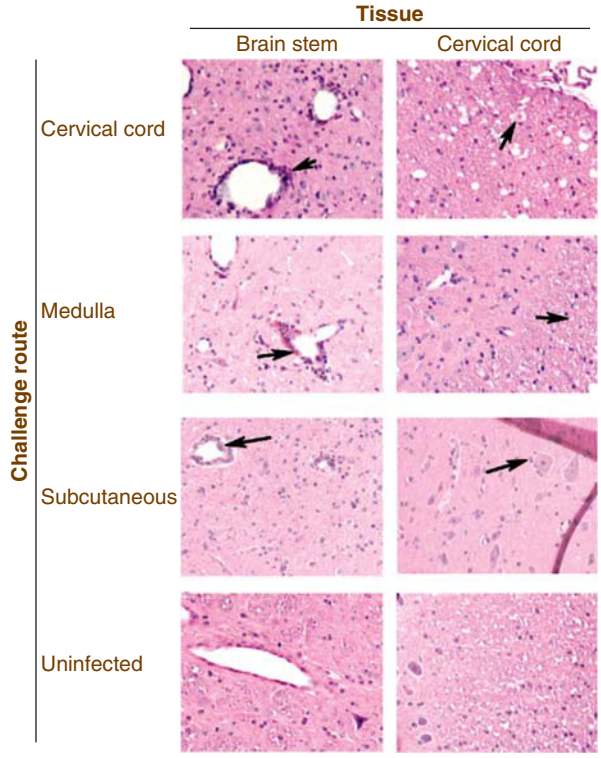


**Figure 4** Examples of the histology from the brain stem and cervical cord from hamsters challenged with WNV in the cervical cord (no. 406), medulla (no. 452), and subcutaneously (no. 301) along with an uninfected hamster. Arrows identify perivascular cuffing, axonal swelling, and lymphocytic cells surrounding neurons. These data correspond to data in Table 1.

spinal cord, since we could not rule out that WNV positivity would be due to extraneurological infection. Therefore, we relied on direct detection of immunoreactive cells in histological sections. This approach of inspecting thin histological sections did have the disadvantage of sampling only a small portion of the candidate tissues for WNV-infected cells, so infectious foci could have been missed. Nevertheless, as the time of infection progressed, WNV-positive neurons were unambiguously identified most consistently in the brain stem and to a lesser extent in the cervical cord, which suggested that infection in these tissues may have caused the EMG suppression.

In an EMG-suppressed animal 3 days after viral challenge, there was no observable neurohistopathology with lymphocytic infiltration or gliosis, as determined by subjective H&E observation in these brain stems. At later days after infection (~day 7), lymphocytosis and gliosis was observed by H&E in subcutaneously injected hamsters. Prior studies have amply demonstrated the role of astrocytes in WNV pathology. Astrocytes can be persistently infected with WNV (Diniz *et al,* 2006), which decreases excitatory amino acid uptake resulting in glutamate excitotoxicity (Blakely *et al,* 2009), and can secrete chemokines and cytotoxic factors that affect neuron viability and microglial production of chemokines (Cheeran *et al,* 2005; Diniz *et al,* 2006; van Marle *et al,* 2007). Direct infection of neurons may also contribute to WNV pathology. The WNV capsid (Oh *et al,* 2006; Yang *et al,* 2002) or nonstructural WNV proteins (Medigeshi *et al,* 2007) can lead to apoptosis of neurons. Depending on the level of infectious doses in cells, necrosis or apoptosis pathways can be involved (Chu and Ng, 2003). Considering the direct infection of neurons and lack of astrocytosis or lymphatic infiltrations 3 days after infection, these data may suggest different phases of pathology. The earliest phase may involve the direct infection of neurons to cause electrophysiological dysfunction, followed by possible death of neurons, or may involve alteration of vagal afferent autonomic function. Later stages of disease would involve infected astrocytes, microglial cells, or reactive T cells to mediate immunopathological disease.

BAER data from this report also supports different phases of pathology. The BAER was selected to determine if generalized brain stem neuropathy was the cause of diaphragmatic EMG suppression. Because deficiencies of BAER were only observed at day 11, which is long after diaphragm EMGs became suppressed, multiple phases of WNV-induced neurological disease are likely. Definitive proof of early and late phases of WNV neurological disease, however, awaits further investigation.

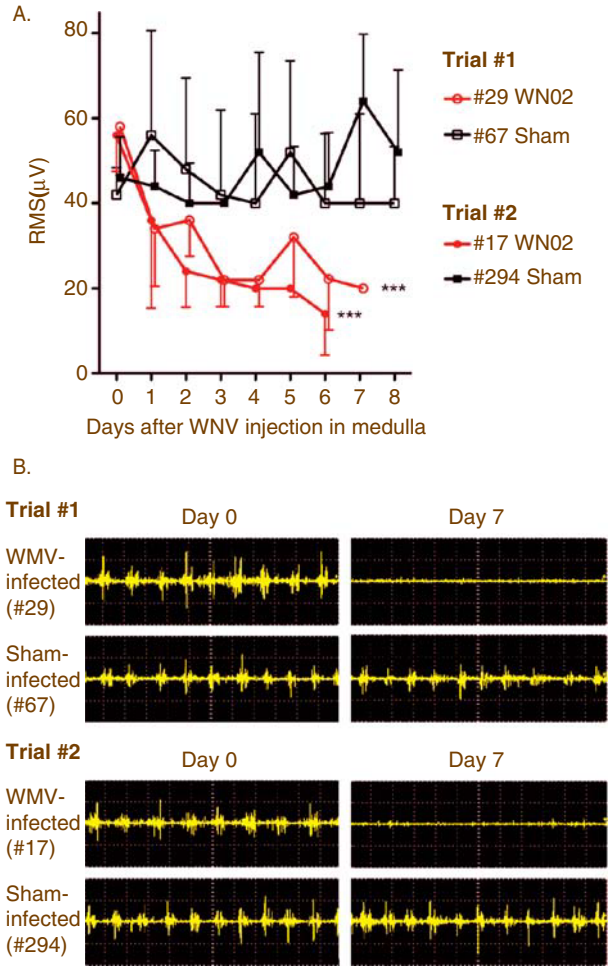


**Figure 5** EMGs of diaphragms from hamsters injected bilaterally with WN02 (TX-113; 2. $8 \times 10^3$ PFU) in the ventrolateral medulla using stereotaxic surgery. (**A**) Root-mean-square (RMS) of EMG amplitudes. (**B**) Representative raw EMG signals at days 0 to 7 after viral challenge from two different trials. Trials 1 and 2 each contained one WNV-injected and one sham-injected hamster. ***$P \leq .001$ of data from day 7 compared to day 0 using two-way ANOVA (Prism 4 for Macintosh; GraphPad Software).

Evidence from these studies indicate that WNV-induced EMG suppression of the diaphragm is neurologically caused, either from direct infection of the brain stem and cervical cord, or from the effects of infection on the afferent vagus nerve controlling autonomic function of the brain stem. This WNV-induced EMG suppression may be analogous to conditions leading to respiratory distress of WNV-infected human patients.

## Materials and methods

*Animals and viruses*

Adult female Syrian golden hamsters were used (Charles River Laboratories). Animals were randomized to treatment groups. This study was conducted in accordance with the approval of the Institutional Animal Care and Use Committee of Utah State University. One New York isolate (NY WNV) (Lanciotti *et al,* 2002; Lanciotti and Kerst, 2001) from crow brain (Davis *et al,* 2004) and one isolate of the emerging dominant genotype (WN02) from bird 113 (TX-113) (Biodefense and Emerging Infectious Research Resources Repository, Manassas, VA) were used. The NY WNV strain was used to increase the probability of EMG dysfunction in the early times of infection before day 6, because the NY strain causes a more robust disease in hamsters as compared to the WN02 strain (Siddharthan *et al,* 2009). WN02 strain was used for animals necropsied after day 6 to increase the numbers of surviving animals for analysis. The viruses were propagated in MA-104 cells and diluted in minimal essential medium (MEM) immediately prior to subcutaneous (s.c.) injection in the groin area with a volume of 100 μl or intracerebrally with 1 μl.

*Histology*

Immunohistochemistry using light microscopy and confocal microscopy was described elsewhere (Morrey *et al,* 2008; Siddharthan *et al,* 2009), in which we performed relevant controls such as absence of the primary antibody, negative controls from uninfected animals, positive controls from kidneys of WNV-infected animals and WNV-infected Vero cells, and confirmation of antibody specificity using three different staining protocols.

For light microscopy, paraffinized sections were used for hematoxylin and eosin (H&E) and detection of WNV envelope. For alkaline phosphatase localization of WNV envelope antigen (Morrey *et al,* 2008), the Ventana NexES IHC Full System (N750-NXIHC-FS; Ventana Medical Systems, Tucson, AZ) was used. The sections were stained with 7H2 monoclonal antibody (mAb) for WNV envelope and detected using Ventana Basic AEC Detection kits (Ventana Medical Systems) according to the manufacturer's instructions and counterstained with hematoxylin. For horseradish peroxidase (HRP) localization of WNV envelope antigen (Wang *et al,* 2009), tissues were incubated with 7H2 anti-WNV mouse mAb at 4°C overnight, incubated with horse anti-mouse immunoglobulin G (IgG) (1:200; BA-2000; Vector Lab) for 2 h at room temperature, and developed with the avidin-biotin-peroxidase complex (ABC) detection system (1:100; Vectastain ABC kit; Vector Lab) for 30 min employing 0.3% hydrogen peroxide and 3,3'-diaminobenzidine (DAB). For confocal microscopy (Siddharthan *et al,* 2009), paraffin sections were processed using primary monoclonal antibody 7H2 against WNV as above, and Alexa-fluor 568 goat anti-mouse IgG antibody for WNV detection. Primary polyclonal anti-neuron-specific enolase (NSE) antibody (Chemicon, Temecula, CA) and Alexa-fluor 488 goat anti-mouse IgG antibody (Molecular Probes, Eugene, OR) were used

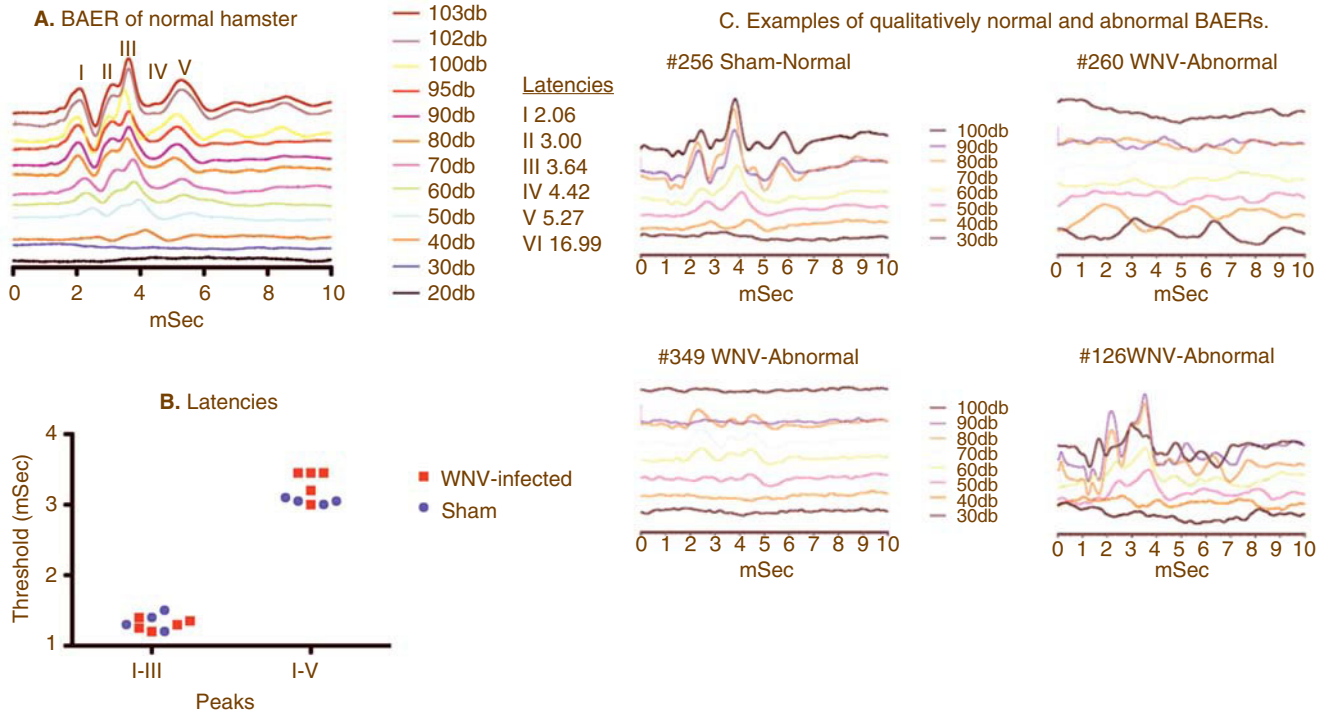


**Figure 6.** Brain auditory evoked response (BAER). (**A**) BAER with peaks in a normal female adult hamster using different decibels (db). (**B**) Latencies between peaks I and III, I and V, and III and V at 7 and 11 days after WNV challenge. (**C**) Examples of normal (no. 256: sham-injected hamster) and qualitatively abnormal (no. 260: WNV-injected; no. 349: WNV-injected; no. 126: WNV-injected hamsters) BAERs obtained after day 11. All of the 15 sham-injected hamsters were normal, but 3 of 12 WNV-injected hamsters were abnormal.

for NSE detection. Stained slides were visualized using a Nikon Eclipse TE300 microscope (Nikon) attached with Lambda DG4 (Sutter Instrument, Novato, CA) and a Bio-Rad MRC 1024 confocal microscope (Bio-Rad, Hercules, CA). A board-certified veterinary pathologist blinded to the identification of the samples examined the H&E-stained sections.

*Cervical cord injection*

Dorsal laminectomy was performed on hamsters (Morrey *et al,* 2008) at the 5th cervical vertebra of the spinal cord. In anesthetized hamsters, the subcutaneous tissues were retracted laterally and the paraspinal muscles were incised immediately lateral to the spinous process. Muscles were scraped from the lamina of the vertebrae with a Friedman Mico Rongeur. The dorsal spinal process of the vertebra was removed. An opening was made in the dura with a 30-gauge needle held at a 20° angle from the horizontal axis of the spine. One microliter of virus ($2.8 \times 10^3$ plaque-forming units [PFU]) was injected into both sides of the spinal cord with a Hamilton syringe held by the arm of a stereotactic apparatus. Both sides were injected. Control animals were sham-infected with viral diluent (minimal essential medium). The dura was sutured with interrupted 4-0 absorbable sutures with a tapered needle (Ethicon). The paraspinal muscles were sutured with 3-0 absorbable sutures and the skin was closed with wound clips. Buprenorphine analgesia (0.05 to 0.1 mg/kg) and the antibiotic Baytril (20 mg/kg) were subcutaneously administered. The hamsters were kept on a heating pad until they regained consciousness.

*Stereotaxic injection of medulla oblongata*

The procedure used for the brain stem injection of hamsters has been described (Mori *et al,* 2002). One microliter of virus ($2.8 \times 10^3$ PFU) was injected at the following stereotaxic coordinates: from the bregma, anterior-posterior: −8.44 mm; mediolateral: ±0.45 mm; dorsoventral: +8.8 mm. Injection was performed on both sides. The coordinates targeted the ventrolateral medulla oblongata near the rostral one-third of the inferior olive nucleus in the hamster.

*Electromyography (EMG) of the diaphragm*

Based on previous procedures (Campbell *et al,* 1995; Fournier and Lewis, 2000), a small incision was made through the abdominal musculature below the left costal margin to expose the abdominal surface of the diaphragm. A pair of 36-gauge Teflon-insulated single-stranded stainless steel wires (AS765 Cooner Wire; Specialty Wire & Cable, Chatsworth, CA) were implanted in the midcostal

region of the left hemidiaphragm. This was accomplished by inserting into the muscle a 26-gauge needle containing the electrode wire with a 1-mm bare tip bent into a hook. When the needle was removed, the electrode remained in the muscle. To secure the electrodes, looped leads of the electrode wires were sutured to intercostal muscles. Additionally, a common ground wire was implanted subcutaneously. The electrode leads were routed subcutaneously to exit on the dorsal surface of the back. Leads were connected to a differential DAM50 amplifier (World Precision Instruments, Sarasota, FL) set at 10K gain and the band-pass filter between 3 Hz and 2 kHz. EMG recordings were monitored on a digital storage oscilloscope (2542BK; BK Precision Electronic Test Instruments, Yorba Linda, CA). EMGs were performed in unanesthetized hamsters placed on a platform ($25 \times 25$ cm$^2$) where 10 consecutive recordings were made. The average root-mean-square (RMS) of the EMG waveform was calculated.

*Brain auditory evoked response (BAER)*
Auditory evoked potentials were recorded with an active electrode at the vertex of the skull and a reference electrode at the bulla of the skull in hamsters. The BAER was recorded using a laptop computer loaded with LabView 8.2 (National Instruments, Austin TX), a NI USB-6212 data acquisition board, a SCB-68 shielded connector block (both from National Instruments), a pair of EARTone 3A insert earphones (EAR Auditory Systems, Indianapolis IN), and an in-line MP3 stereo amplifier (Boostaroo, Nunica MI). This system was programmed to produce auditory stimuli 0.1 ms in duration consisting of a 14-kHz tone and the stimulus was repeated at a rate of 11 Hz. The input for the Labview/computer BAER system came from a DAM-50 2 channel amplifier (World Precision Instruments) via acupuncture needles (40 G) soldered to a set of shielded EMG cables (Chalgren, Gilroy CA). LabView was programmed to capture 500 evoked responses and then compute their average. The animal and the amplifier was placed inside a 24-inch $\times$ 24-inch custom-made copper Faraday cage (BioQuip Products, Rancho Dominguez, CA) lined with home theater noise reducing rubber sheet and pyramidal foam. The outside was covered with home theater acoustic ceiling tiles (Acoustical Solutions, Richmond, VA). To analyze the data, 10-db steps of increasing decibels (db) of sound from 30 to 100 db were used to elicit responses to measure the thresholds of peaks I and V. Eighty decibels of sound were used to measure the latency between peaks I and III and I and V.

***Declaration of interest:*** The authors report no conflicts of interest. The authors alone are responsible for the content and writing of the paper.

## References

Atkinson W, Hamborsky J, McIntyre L, Wolfe S (eds). (2007). Poliomyelitis. In: *Epidemiology and Prevention of Vaccine-Preventable Diseases*, (The Pink Book), pp 101–114, Centers for Disease Control and Prevention, Public Health Foundation, Washington DC.

Blakely PK, Kleinschmidt-DeMasters BK, Tyler KL, Irani DN (2009). Disrupted glutamate transporter expression in the spinal cord with acute flaccid paralysis caused by West Nile virus infection. *J Neuropathol Exp Neurol* **68:** 1061–1072.

Campbell C, Weinger MB, Quinn M (1995). Alterations in diaphragm EMG activity during opiate-induced respiratory depression. *Respir Physiol* **100:** 107–117.

Cantile C, Del Piero F, Di Guardo G, Arispici M (2001). Pathologic and immunohistochemical findings in naturally occuring West Nile virus infection in horses. *Vet Pathol* **38:** 414–421.

Cheeran MC, Hu S, Sheng WS, Rashid A, Peterson PK, Lokensgard JR (2005). Differential responses of human brain cells to West Nile virus infection. *J NeuroVirol* **11:** 512–524.

Chu JJ, Ng ML (2003). The mechanism of cell death during West Nile virus infection is dependent on initial infectious dose. *J Gen Virol* **84:** 3305–3314.

Davis CT, Beasley DW, Guzman H, Siirin M, Parsons RE, Tesh RB, Barrett AD (2004). Emergence of attenuated West Nile virus variants in Texas, 2003. *Virology* **330:** 342–350.

Diniz JA, Da Rosa AP, Guzman H, Xu F, Xiao SY, Popov VL, Vasconcelos PF, Tesh RB (2006). West Nile virus infection of primary mouse neuronal and neuroglial cells: the role of astrocytes in chronic infection. *Am J Trop Med Hyg* **75:** 691–696.

Doron SI, Dashe JF, Adelman LS, Brown WF, Werner BG, Hadley S (2003). Histopathologically proven poliomyelitis with quadriplegia and loss of brainstem function due to West Nile virus infection. *Clin Infect Dis* **37:** e74–e77.

Dubreuil V, Thoby-Brisson M, Rallu M, Persson K, Pattyn A, Birchmeier C, Brunet JF, Fortin G, Goridis C (2009). Defective respiratory rhythmogenesis and loss of central chemosensitivity in Phox2b mutants targeting retrotrapezoid nucleus neurons. *J Neurosci* **29:** 14836–14846.

Focosi D, Kast RE, Maggi F, Vatteroni L, Ceccherini-Nelli L, Petrini M (2007). Hypothesis: central nervous system delivery of cyclosporine A for therapy of progressive multifocal leukoencephalopathy. *J Clin Virol* **39:** 156–158.

Fournier M, Lewis MI (2000). Functional, cellular, and biochemical adaptations to elastase-induced

emphysema in hamster medial scalene. *J Appl Physiol* **88:** 1327–1337.

Fratkin JD, Leis AA, Stokic DS, Slavinski SA, Geiss RW (2004). Spinal cord neuropathology in human West Nile virus infection. *Arch Pathol Lab Med* **128:** 533–537.

Gaultier C, Amiel J, Dauger S, Trang H, Lyonnet S, Gallego J, Simonneau M (2004). Genetics and early disturbances of breathing control. *Pediatr Res* **55:** 729–733.

Goehler LE, Erisir A, Gaykema RP (2006). Neural-immune interface in the rat area postrema. *Neuroscience* **140:** 1415–1434.

Goehler LE, Gaykema RP, Opitz N, Reddaway R, Badr N, Lyte M (2005). Activation in vagal afferents and central autonomic pathways: early responses to intestinal infection with Campylobacter jejuni. *Brain Behav Immun* **19:** 334–344.

Gonzalez C, Almaraz L, Obeso A, Rigual R (1994). Carotid body chemoreceptors: from natural stimuli to sensory discharges. *Physiol Rev* **74:** 829–898.

Gowen BB, Smee DF, Wong MH, Hall JO, Jung KH, Bailey KW, Stevens JR, Furuta Y, Morrey JD (2008). Treatment of late stage disease in a model of arenaviral hemorrhagic fever: T-705 efficacy and reduced toxicity suggests an alternative to ribavirin. *PLoS ONE* **3:** e3725.

Hermann GE, Rogers RC (2009). TNF activates astrocytes and catecholaminergic neurons in the solitary nucleus: implications for autonomic control. *Brain Res* **1273:** 72–82.

Hoffman LF, Horowitz JM (1984). Far-field brainstem responses evoked by vestibular and auditory stimuli exhibit increases in interpeak latency as brain temperature is decreased. *Physiologist* **27:** S89–S90.

Jiang ZD, Wu YY, Wilkinson AR (2009). Age-related changes in BAER at different click rates from neonates to adults. *Acta Paediatr* **98:** 1284–1287.

Lanciotti RS, Ebel GD, Deubel V, Kerst AJ, Murri S, Meyer R, Bowen M, McKinney N, Morrill WE, Crabtree MB, Kramer LD, Roehrig JT (2002). Complete genome sequences and phylogenetic analysis of West Nile virus strains isolated from the United States, Europe, and the Middle East. *Virology* **298:** 96–105.

Lanciotti RS, Kerst AJ (2001). Nucleic acid sequence-based amplification assays for rapid detection of West Nile and St. Louis encephalitis viruses. *J Clin Microbiol* **39:** 4506–4513.

Medigeshi GR, Lancaster AM, Hirsch AJ, Briese T, Lipkin WI, Defilippis V, Fruh K, Mason PW, Nikolich-Zugich J, Nelson JA (2007). West Nile virus infection activates the unfolded protein response, leading to CHOP induction and apoptosis. *J Virol* **81:** 10849–10860.

Mori I, Liu B, Hossain MJ, Takakuwa H, Daikoku T, Nishiyama Y, Naiki H, Matsumoto K, Yokochi T, Kimura Y (2002). Successful protection by amantadine hydrochloride against lethal encephalitis caused by a highly neurovirulent recombinant influenza A virus in mice. *Virology* **303:** 287–296.

Morrey JD, Day CW, Julander JG, Olsen AL, Sidwell RW, Cheney CD, Blatt LM (2004). Modeling hamsters for evaluating West Nile virus therapies. *Antiviral Res* **63:** 41–50.

Morrey JD, Siddharthan V, Olsen AL, Wang H, Julander JG, Hall JO, Li H, Nordstrom JL, Koenig S, Johnson S, Diamond MS (2007). Defining the limit of effective treatment for West Nile virus neurological infection with a humanized neutralizing monoclonal antibody. *Antimicrob Agents Chemother* **51:** 2396–2402.

Morrey JD, Siddharthan V, Wang H, Hall JO, Skirpstunas RT, Nordstrom JL, Koenig S, Johnson S, Diamond MS (2008). West Nile virus-induced acute flaccid paralysis is prevented by monoclonal antibody treatment even after infection of spinal cord neurons. *J NeuroVirol* **14:** 152–163.

Oh W, Yang MR, Lee EW, Park KM, Pyo S, Yang JS, Lee HW, Song J (2006). Jab1 mediates cytoplasmic localization and degradation of west nile virus capsid protein. *J Biol Chem* **281:** 30166–30174.

Okada Y, Kuwana S, Chen Z, Ishiguro M, Oku Y (2009). The central respiratory chemoreceptor: where is it located?-Invited article. *Adv Exp Med Biol* **648:** 377–385.

Petropoulou KA, Gordon SM, Prayson RA, Ruggierri PM (2005). West Nile virus meningoencephalitis: MR imaging findings. *AJNR Am J Neuroradiol* **26:** 1986–1995.

Rudzinski E, Kapur RP (2010). PHOX2B Immunolocalization of the candidate human retrotrapezoid nucleus. *Pediatr Dev Pathol*: In press.

Samuel MA, Morrey JD, Diamond MS (2006). Caspase-3 dependent cell death of neurons contributes to the pathogenesis of West Nile virus encephalitis. *J Virol* **81:** 2614–2623.

Sejvar JJ, Bode AV, Marfin AA, Campbell GL, Ewing D, Mazowiecki M, Pavot PV, Schmitt J, Pape J, Biggerstaff BJ, Petersen LR (2005). West Nile virus-associated flaccid paralysis. *Emerg Infect Dis* **11:** 1021–1027.

Sejvar JJ, Bode AV, Marfin AA, Campbell GL, Pape J, Biggerstaff BJ, Petersen LR (2006). West Nile Virus-associated flaccid paralysis outcome. *Emerg Infect Dis* **12:** 514–516.

Shrestha B, Gottlieb D, Diamond MS (2003). Infection and injury of neurons by West Nile encephalitis virus. *J Virol* **77:** 13203–13213.

Siddharthan V, Wang H, Motter NE, Hall JO, Skinner RD, Skirpstunas RT, Morrey JD (2009). Persistent West Nile virus associated with a neurological sequela in hamsters identified by motor unit number estimation. *J Virol* **83:** 4251–4261.

Siirin MT, Duan T, Lei H, Guzman H, da Rosa AP, Watts DM, Xiao SY, Tesh RB (2007). Chronic St. Louis encephalitis virus infection in the golden hamster (Mesocricetus auratus). *Am J Trop Med Hyg* **76:** 299–306.

Tonry JH, Xiao SY, Siirin M, Chen H, da Rosa AP, Tesh RB (2005). Persistent shedding of West Nile virus in urine of experimentally infected hamsters. *Am J Trop Med Hyg* **72:** 320–324.

van Marle G, Antony J, Ostermann H, Dunham C, Hunt T, Halliday W, Maingat F, Urbanowski MD, Hobman T,

Peeling J, Power C (2007). West Nile virus-induced neuroinflammation: glial infection and capsid protein-mediated neurovirulence. *J Virol* **81:** 10933–10949.

Wang H, Siddharthan V, Hall JO, Morrey JD (2009). West Nile virus preferentially transports along motor neuron axons after sciatic nerve injection of hamsters. *J NeuroVirol* **4:** 1–7.

Woischneck D, Kapapa T, Heissler HE, Reissberg S, Skalej M, Firsching R (2009). Respiratory function after lesions in medulla oblongata. *Neurol Res* **31:** 1019–1022.

Wu X, Lu L, Guzman H, Tesh RB, Xiao SY (2008). Persistent infection and associated nucleotide changes of West Nile virus serially passaged in hamsters. *J Gen Virol* **89:** 3073–3079.

Yang JS, Ramanathan MP, Muthumani K, Choo AY, Jin SH, Yu QC, Hwang DS, Choo DK, Lee MD, Dang K, Tang W, Kim JJ, Weiner DB (2002). Induction of Inflammation by West Nile virus capsid through the caspase-9 apoptotic pathway. *Emerg Infect Dis* **8:** 1379–1384.

This paper was first published online on Early Online on 15 July 2010.